# Nanosecond molecular relaxations in lipid bilayers studied by high energy-resolution neutron scattering and *in situ* diffraction

Maikel C. Rheinstädter* and Tilo Seydel
*Institut Laue-Langevin, 6 rue Jules Horowitz, Boîte Postale 156, 38042 Grenoble Cedex 9, France*

Tim Salditt
*Institut für Röntgenphysik, Friedrich-Hund Platz 1, 37077 Göttingen, Germany*
(Received 10 July 2006; published 10 January 2007)

We report a high energy-resolution neutron backscattering study to investigate slow motions on nanosecond time scales in highly oriented solid-supported phospholipid bilayers of the model system deuterated 1,2-dimyristoyl-sn-glycero-3-phosphatidylcholine, hydrated with heavy water. Wave-vector-resolved quasielastic neutron scattering is used to determine relaxation times $\tau$, which can be associated with different molecular components, i.e., the lipid acyl chains and the interstitial water molecules in the different phases of the model membrane system. The inelastic data are complemented by both energy-resolved and energy-integrated *in situ* diffraction. From a combined analysis of the inelastic data in the energy and time domains, the corresponding character of the relaxation, i.e., the exponent of the exponential decay, is also determined. From this analysis we quantify two relaxation processes. We associate the fast relaxation with translational diffusion of lipid and water molecules while the slow process likely stems from collective dynamics.

DOI: 10.1103/PhysRevE.75.011907 PACS number(s): 87.14.Cc, 87.16.Dg, 83.85.Hf, 83.10.Mj

## I. INTRODUCTION

Inelastic scattering techniques give a wave-vector-resolved access to dynamical properties, i.e., excitation frequencies or relaxation rates can be quantified at different internal length scales. This is important to associate the dynamics with individual modes of motion. A unique advantage lies in the simultaneous access to both structural and dynamical properties by measuring the scattering $S(\vec{Q},\omega)$ as a function of wave vector transfer $\vec{Q}$ and energy transfer $\omega$. We here report on $\mu$eV energy-resolved spectra in the model membrane system deuterated 1,2-dimyristoyl-sn-glycero-3-phosphatidylcholine (DMPC-d54), achieved by the neutron backscattering technique. By analyzing the corresponding $Q$ dependence, we simultaneously probe low energetic density fluctuations of lipid acyl chains and interstitial water molecules, i.e., the water layer in between the stacked membranes.

The spectrum of fluctuations in biomimetic and biological membranes covers a large range of time and length scales [1–9], ranging from the long wavelength undulation and bending modes of the bilayer with typical relaxation times of nanoseconds and lateral length scales of several hundreds lipid molecules to the short wavelength density fluctuations in the picosecond range on nearest neighbor distances of lipid molecules. Local dynamics in lipid bilayers, i.e., dynamics of individual lipid molecules which as vibration, rotation, libration (hindered rotation), and diffusion, has been investigated by, e.g., incoherent neutron scattering [1–5] and nuclear magnetic resonance [10,11] to determine the short wavelength translational and rotational diffusion constant. Collective undulation modes have been investigated using neutron spin-echo spectrometers [4,5,12,13] and dynamical light scattering [14–16]. Information about fluctuations on mesoscopic length scales can also be inferred from x-ray line-shape analysis [17,18] in isotropic lipid dispersions. Off-specular x-ray and neutron reflectivity from aligned phases presents the additional advantage that the components of the scattering vector $\vec{Q}$ can be projected onto the symmetry axis of the membrane [9,18–22]. In both examples, the time-averaged elastic scattering is studied, and information on, e.g., elasticity properties and interaction forces can be obtained. Only recently have the first inelastic scattering experiments in phospholipid bilayers to determine collective motions of the lipid acyl chains and in particular the short wavelength dispersion relation been performed using inelastic x-ray [23] and neutron [24] scattering techniques. While here fast propagating sound modes in the picosecond time range have been quantified, the present paper deals with slow nanosecond relaxation times on length scales of nearest neighbor distances of phospholipid acyl chains and water molecules, i.e., the slow dynamics of melting (diffusion) and collective movements (most likely undulations) of the lipid and water backbone. We have selected the neutron backscattering technique for this study since the dynamical modes at high $q_{\|}$ (the in-plane component of the scattering vector $\vec{Q}$) are too fast to be accessed by x-ray photon correlation spectroscopy (XPCS) and the lateral length scales are too small to be resolved by dynamic light scattering or the neutron spin-echo (NSE) technique. Note that the feasibility of wave-vector-resolved backscattering experiments in oriented membrane systems to study freezing of lipid acyl chains and water molecules has been established only recently [25]. In this work we present the unprecedented determination of relaxation rates from $Q$-resolved backscattering quasielastic neutron scattering data in phospholipid bilayers,

*Present address: Department of Physics and Astronomy, University of Missouri–Columbia, Columbia, MO 65211, USA. Electronic address: RheinstadterM@missouri.edu

 

combined with *in situ* diffraction to assign the relaxation times to the respective phases of the model membranes. These measurements are carried out in aligned phases to preserve the unique identification of modes on the basis of the parallel and perpendicular components of the scattering vector $\vec{Q}$, i.e., the lateral momentum transfer in the plane of the bilayers $q_{\|}$, and the reflectivity $q_z$.

## II. EXPERIMENT

Partially (acyl chain) deuterated DMPC-d54 was obtained from Avanti Polar Lipids. In the case of single membranes the inelastic neutron scattering signal is by far not sufficient for a quantitative study of the inelastic scattering. Highly oriented multilamellar membrane stacks of several thousands of lipid bilayers were therefore prepared by spreading a lipid solution of typically 25 mg/ml lipid in trifluoroethylene-chloroform (1:1) on 2 in. silicon wafers, followed by subsequent drying in vacuum and hydration from $D_2O$ vapor [26], resulting in a structure of smectic *A* symmetry. Twenty such wafers separated by small air gaps were combined and aligned with respect to each other to create a "sandwich sample" consisting of several thousands of highly oriented lipid bilayers (total mosaicity about 0.5°), with a total mass of about 400 mg of deuterated DMPC. The mosaicity is composed of the alignment of the bilayers within the stack on one wafer and of the orientation of different wafers with respect to each other, and was also determined experimentally [13]. It follows from an optimized sample preparation and the spatial alignment and orientation of the wafers in the sample holder. The sample was mounted in a hermetically sealed aluminum container within a cryostat and hydrated from $D_2O$ vapor. Saturation of the vapor in the voids around the lipids was assured by placing a piece of pulp soaked in $D_2O$ within the sealed sample container. The pulp was shielded by cadmium to exclude any parasitic contribution to the scattering. The hydration was not controlled but we allowed the sample to equilibrate for 10 h at room temperature before the measurements. The large beam divergence as compared to reflectometers did not allow as to determine the corresponding $d_z$ spacing simultaneously with sufficient accuracy to determine the swelling state of the membrane stack *in situ*. Measurements of the same sample on a diffractometer gave a value of $d_z=54$ Å at $T=30°$, corresponding to a relative humidity of 99.6% [27].

The experiment was carried out at the cold neutron backscattering spectrometer IN16 [28] at the Institut Laue-Langevin (ILL) in its standard setup with Si(111) monochromator and analyzer crystals corresponding to an incident and analyzed neutron energy of 2.08 meV ($\lambda=6.27$ Å) resulting in a high resolution in energy transfer of about 0.9 $\mu$eV full width at half maximum FWHM. An energy transfer of $-15<E<+15$ $\mu$eV can be scanned by varying the incident energy by Doppler-shifting the incident neutron energy through an adequate movement of the monochromator crystal. Twenty detectors in exact backscattering with respect to the analyzer crystals covering an angular width of 6.5° each have been used. Note that the maximum of the static *bulk* water correlation peak at about $q_{\|}\approx 2$ Å$^{-1}$ is not accessible because of simple geometrical reasons. The setup is therefore more sensitive for detecting *amorphous* water with slightly larger nearest neighbor distances, as is expected to occur in the water layers of the stacked bilayers. A separate line of 160 energy-integrating diffraction detectors—mounted 24.4° below the (horizontal) scattering plane—with an angular width of 1° each—allows us to simultaneously detect structural changes with a much higher $q_{\|}$ resolution.

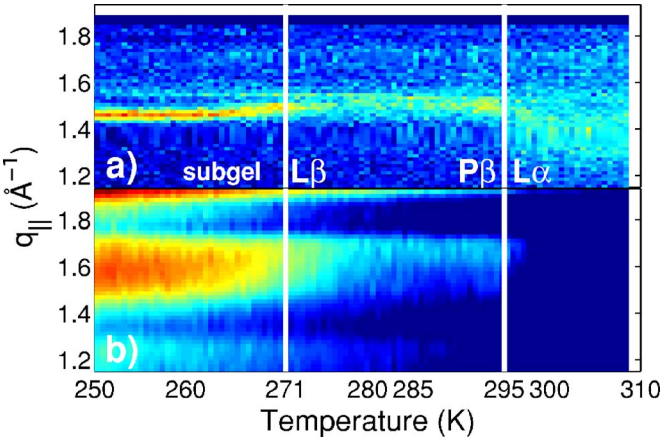


FIG. 1. (Color online). (a) Energy-integrated diffraction for temperatures $250<T<310$ K with a temperature resolution of $\Delta T\approx 0.3$ K (normalized to acquisition time). $q_{\|}$ is the in-plane component of the scattering vector $\vec{Q}$. The phase boundaries for gel ($L\beta$), ripple ($P\beta'$), and fluid phase ($L\alpha$) as defined by structural changes, i.e., the change of peak position and width, are marked by the solid white lines. (b) "True" elastic scattering, measured with an energy resolution of 0.9 $\mu$eV. The phase transitions are also visible in the energy-resolved diffraction data by following the melting at the lipid acyl chain and water positions. Data are normalized to monitor detector efficiency, normalized to the scattering signal of a 2-mm-thick vanadium plate oriented at 135° with respect to the incoming beam. Please note that no absorption correction has been done. For geometrical reasons the diffraction detectors have a lower maximum $q_{\|}$ than the backscattering detectors.

## III. RESULTS FROM NEUTRON DIFFRACTION

We simultaneously performed two types of diffraction measurements, namely, energy-resolved and energy-integrated measurements. Note that the additional diffraction detectors integrate very well over low lying excitations and relaxations. Figure 1(a) shows an energy-integrated diffraction pattern for $1.1<q_{\|}<1.85$ Å$^{-1}$. From the temperature dependence of the inter-acyl-chain correlation peak at $q_{\|}\approx 1.4$ Å$^{-1}$ we assign the temperature of the main transition ($P\beta'$-$L\alpha$) to $T=295$ K. The transition temperature of the gel to ripple phase ($L\beta$-$P\beta'$) is difficult to determine from the data, also because the nearest neighbor acyl peak is not the most sensitive measure of the gel to ripple transition, but it can be estimated to about 285 K. $T_{fw}=271$ K marks the freezing temperature of the amorphous water layer in between the stacked membranes [25]. The correlation peak gradually shifts to smaller $q_{\|}$ values below $T_{fw}$ until about 264 K. In the range $264<T<271$ K water migrates out the

bilayer stacks to freeze as bulk water, as discussed in detail in Ref. [25]. The energy resolved pattern in Fig. 1(b) sheds light on the melting process of lipid acyl chains and water and perfectly reproduces the results previously reported in [25] (the difference being the larger number of detectors). Only structures which are static with respect to the energy resolution of 0.9 $\mu$eV, which corresponds to motions slower than approximately 4 ns, are detected as elastic when using the energy-resolving backscattering detectors. Changes in this intensity may arise from either structural or dynamical changes, i.e., shifts of correlation peaks or freezing or melting of dynamical modes. Elastic intensity at the water detectors rises at $T<271$ K; at the acyl chain position there is an elastic contribution below 295 K, the temperature of the main transition. A further increase occurs when entering the gel ($L\beta$) phase indicating the high degree of dynamics in the ripple ($P\beta'$) phase. Note that there is very little elastic contribution in the fluid phases pointing out that the intensity usually measured in diffraction experiments stems predominantly from low lying fluid excitations and quasielastic scattering.

## IV. INELASTIC SCATTERING

Based on the diffraction patterns we have recorded inelastic scans at temperatures of $T=250$, 280, 292 K and at 310 K, far in the fluid $L\alpha$ phase of the model membranes. Additional scans in the regime of critical swelling ($T=296$, 297, 299, and 303 K) have also been taken. The results for the acyl chain ($q_{\|}\approx 1.4$ Å$^{-1}$) and the water position ($q_{\|}\approx 1.9$ Å$_{-1}$) are depicted in Fig. 2. At 250 K, both $q_{\|}$ positions are well fitted by a single Lorentzian, i.e., a single relaxation process with an energy width (FWHM) $\Delta\omega$ and corresponding relaxation time $\tau=2\pi/\Delta\omega$. For temperatures above 280 K for the water and above 292 K for the acyl chains two Lorentzians are needed to describe the data. Although the Lorentzians describe the energy spectra, small deviations from the fits are visible pointing to deviations from single exponential relaxations. A detailed analysis in energy space is difficult and would mean to add more Lorentzian or mix Lorentzian and Gaussian peak profiles with the risk of being physically meaningless. To further characterize the relaxation processes the data have been Fourier transformed (using the MATLAB FFT algorithm) to determine the exponent $\beta$ of the corresponding exponential decays in time domain, $\exp[-(t/\tau)^{\beta}]$, from fits to the intermediate scattering function $I(q_{\|},t)$, as shown in Fig. 3. With increasing temperature there is a relaxation step moving into the time window at the two $q_{\|}$ positions, respectively. Because of the limited dynamical range of 15 $\mu$eV, the shortest time accessible is about 0.2 ns and the faster process is already partially out of the accessible time window, i.e., the quasielastic broadening is slightly broader than the energy window. No exponent could therefore be reliably determined for the fast process. The resulting relaxation times $\tau_{0,1}$ and the corresponding exponent of the slow process, $\beta_0$, are depicted in Figs. 4(a) and 4(b) for all measured temperatures. To gain reliable fitting parameters for $\tau$ and $\beta$, the relaxation times $\tau_{0,1}$ have been determined from the energy spectra

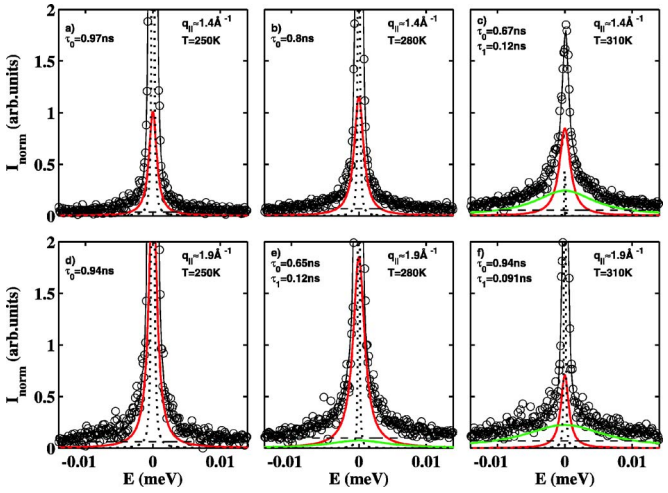


FIG. 2. (Color online) Inelastic scans at the lipid chain ($q_{\|}\approx 1.4$ Å$^{-1}$) and water ($q_{\|}\approx 1.9$ Å$^{-1}$) positions for temperatures $T=250$, 280, and 310 K. Detectors have been grouped to increase counting statistics. The inter-acyl- chain correlation peak is measured by detectors 9–13, which cover a $q_{\|}$ range of $1.20<q_{\|}<1.60$ Å$^{-1}$. The water contribution is detected by detectors 17–20 covering $1.78<q_{\|}<1.94$ Å$^{-1}$. As a model, up to two Lorentzian peak profiles [(red and green) thick solid lines] to describe the quasielastic broadening and a Dirac function (dotted line) to describe the elastic intensity were assumed. This model was convoluted with the measured resolution function obtained from a vanadium standard. A flat background (dashed line) was subsequently added and the result was fitted (fit result, black solid line) to the data (circles). A flat background may arise from fast processes far beyond the accessible energy window of the spectrometer. The thus obtained relaxation times are given in the figures. The calibration error of the energy scale is approx.3%.

$S(q_{\|},\omega)$ in Fig. 2 because this gives the highest accuracy and stability. The $\tau$ values have then been fixed for the fits of the exponential decay in the time domain. $\beta$ is determined from the fits to $I(q_{\|},t)$ in Fig. 3. The two processes at the two $q_{\|}$ positions show distinctly different relaxation times and temperature dependencies. While the fast process has constant times of about 0.1 ns, the slow process starts at about 1 ns at 250 K and becomes faster as approaching the main phase transition at 295 K. Note that because of the limited dynamical range the accuracy in determining the fast relaxation time $\tau_1$ is also limited and we cannot exclude a temperature dependence of the fast process. While for the fast branches no exponent can be determined for the same reason, the slow processes show a stretched exponential character at low temperatures and turn to single exponential when the corresponding correlations melt at the lipid (main transition) and water melting temperature, respectively.

## V. DISCUSSION

From the inelastic neutron data we quantify two relaxation times. We argue that the corresponding processes stem from collective motions of the lipid acyl chains and interstitial water molecules, respectively, rather than from local dynamics. By selective deuteration of the chains and hydration

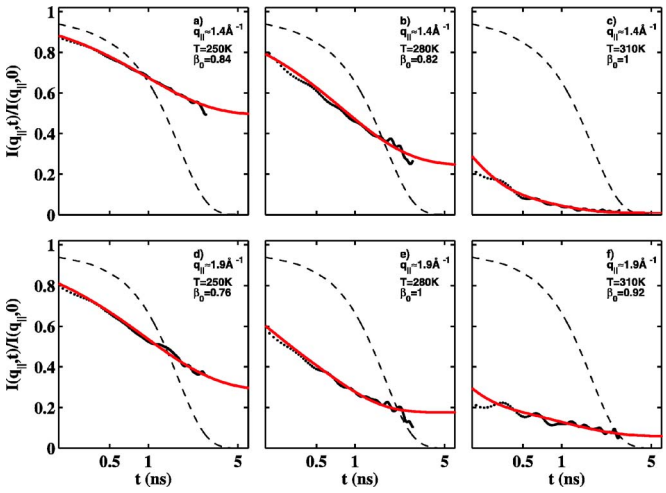


FIG. 3. (Color online) Corresponding Fourier-transformed energy space data (power spectra) from Fig. 2 points), divided by an analytical description of the vanadium resolution. The thus obtained intermediate scattering function $I(q_\parallel,t)/I(q_\parallel,0)$ is shown together with the fits [gray (red) solid line] of two exponential decays $I(q_\parallel,t)/I(q_\parallel,0)=(A_0-A_1)\exp\{-[t/\tau_0(q_\parallel)]^{\beta 0}\}+y_1+(A_1-y_1)\exp\{-[t/\tau_1(q_\parallel)]^{\beta 1}\}$. The values for $\tau_{0,1}$ have been fixed from the energy scans and only the exponents $\beta_{0,1}$ and the amplitudes $A_{0,1}$ have been fitted. The obtained values for $\beta_0$ are given in the figures. The vanadium resolution is also plotted (dashed line). While the data at 250 K are well described by one exponential decay, two decays are needed at higher temperatures.

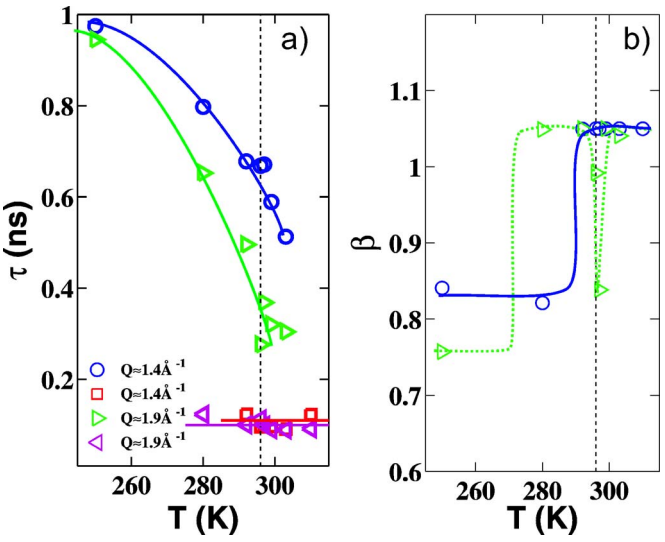


FIG. 4. (Color online) (a) Relaxation times at the lipid chain and the water position for all measured temperatures as determined from fits to the quasielastic data in Fig. 2. (b) Exponents of the exponential decay as determined from fits of the intermediate scattering function from Fig. 3. Solid lines are guides to the eye.

from $D_2O$ vapor, coherent motions are strongly enhanced over other contributions to the inelastic scattering cross section.[1] The fast process $\tau_1$ disappears below the freezing temperature of the lipids ($P\beta'$ phase) respective water molecules ($T<T_{fw}=271$ K) and might therefore be due to (collective) translational diffusion of lipids and water. The slow process with relaxation times $\tau_0$ is measured down to the lowest temperatures of $T=250$ K and most likely probes collective dynamics, i.e., neighboring lipid and water molecules participating in slow mesoscopic dynamics. However, to further characterize this process, $q_\parallel$-dependent data are needed to determine the corresponding dispersion relation and compare to theoretical models. It is speculated in the literature that the minimum in the dispersion relation of the collective fast propagating modes at the nearest neighbor distances of lipid acyl chains (as determined in Refs. [23,24]) is related to transport phenomena within and across the bilayers. The relaxation found in the present paper on the same length but distinctly different time scale might be relevant to establish such a model of *phonon-assisted diffusion* in membranes, which would be of particular interest in membrane biophysics and biotechnology applications.

[1]Neutron scattering data may include contributions from coherent and incoherent scattering, i.e., from pair- and autocorrelated scattering (collective and local or diffusive modes). While in protonated samples the incoherent scattering is usually dominant and the time-autocorrelation function of individual scatterers is accessible in neutron scattering experiments, (partial) deuteration emphasizes the coherent scattering and gives access to collective motions by probing the pair-correlation function.

The slow relaxations at the acyl chain and the water position both show a decrease of relaxation times towards the main transition of the phospholipids. The relaxation time of the fast branch with $\tau\approx 0.1$ ns that we attribute to translational diffusion is temperature independent within the experimental accuracy, which is slightly limited by the maximum achievable energy transfer. Note that the diffusion time measured here can be interpreted as time for hopping processes to nearest neighbor sites. Such a process needs a free neighboring site but does not necessarily give information about the mobility of these holes (free surface or volume) which would be important for macroscopic diffusion. The corresponding time scales and diffusion constants might therefore be distinctly different. From measurements with a higher dynamical range, the energy barrier of this excitation could probably be determined from the temperature dependent hopping times using Arrhenius or Vogel-Fulcher laws.

The $\beta$ exponents in Fig. 4(b) start at values $\beta<1$ at low temperatures. Structural inhomogeneities and heterogeneous interactions obviously lead to a local relaxation dynamics and to stretched ($\beta<1$) exponentials. When entering the fluid phase at $T_m$, the lipid relaxations ($q_\parallel\approx 1.4$ Å$^{-1}$) turn into single exponential, as can be expected for a diffusive, fluidlike motion of the particles. At the water position ($q_\parallel\approx 1.9$ Å$^{-1}$), the transition from stretched to single exponential occurs between 250 and 280 K, most likely at the water freezing or melting temperature $T_{fw}=271$ K, as speculated and indicated in the figure. A striking feature is that in the range of critical swelling, the water relaxations become again stretched, which might be related to the expansion of the water layer leading to the well known anomalous swelling of phospholipid bilayers close to the main transition [27,29].

## VI. CONCLUSION

In conclusion, using the neutron backscattering technique, we have determined $q_{\parallel}$-dependent relaxation times at different temperatures in the model membrane system DMPC that we attribute to lipid acyl chains and interstitial water molecules. *In situ* diffraction allowed us to assign the temperatures to the different phases of the bilayers. A combined data analysis in the energy and time domains allowed us to quantify relaxation times of two processes and determine the exponents $\beta$ of the exponential decays. The fast process is attributed to diffusion while the slow process likely stems from collective dynamics. We find stretched exponential relaxations at low temperatures. The relaxations turn into single exponential above the corresponding melting temperatures of lipid and water molecules.

Future experiments, which will include a selective deuteration of the acyl chains and the membrane water, respectively, will allow to mask different types of mobility and hopefully deduce complete dispersion relations of the different molecular components in the different phases of the phospholipid bilayers. Compared to NSE and XPCS, large $Q$ values can easily be obtained. The current drawback of the technique is the limited dynamical range on high flux spectrometers which hopefully will be overcome in next generation neutron sources and backscattering spectrometers. Our study also points to the wealth of new information that can be explored with the membrane backscattering technique.

## ACKNOWLEDGMENTS

We acknowledge T. Gronemann (Institut für Röntgenphysik, Göttingen) for help with the sample preparation, M. Elender (ILL) for technical and engineering support, and the ILL for the allocation of beam time.

[1] S. König, W. Pfeiffer, T. Bayerl, D. Richter, and E. Sackmann, J. Phys. II **2**, 1589 (1992).
[2] S. König, E. Sackmann, D. Richter, R. Zorn, C. Carlile, and T. Bayerl, J. Chem. Phys. **100**, 3307 (1994).
[3] S. König, T. Bayerl, G. Coddens, D. Richter, and E. Sackmann, Biophys. J. **68**, 1871 (1995).
[4] W. Pfeiffer, T. Henkel, E. Sackmann, and W. Knorr, Europhys. Lett. **8**, 201 (1989).
[5] W. Pfeiffer, S. König, J. Legrand, T. Bayerl, D. Richter, and E. Sackmann, Europhys. Lett. **23**, 457 (1993).
[6] E. Lindahl and O. Edholm, Biophys. J. **79**, 426 (2000).
[7] *Structure and Dynamics of Membranes*, edited by R. Lipowsky and E. Sackmann, Handbook of Biological Physics, Vol. 1 (Elsevier, Amsterdam, 1995).
[8] T. Bayerl, Curr. Opin. Colloid Interface Sci. **5**, 232 (2000).
[9] T. Salditt, Curr. Opin. Colloid Interface Sci. **5**, 19 (2000).
[10] A. Nevzorov and M. Brown, J. Chem. Phys. **107**, 10288 (1997).
[11] M. Bloom and T. Bayerl, Can. J. Phys. **73**, 687 (1995).
[12] T. Takeda, Y. Kawabata, H. Seto, S. Komura, S. Gosh, M. Nagao, and D. Okuhara, J. Phys. Chem. Solids **60**, 1375 (1999).
[13] M. C. Rheinstädter, W. Häussler, and T. Salditt, Phys. Rev. Lett. **97**, 048103 (2006).
[14] R. Hirn, T. Bayerl, J. Rädler, and E. Sackmann, Faraday Discuss. **111**, 17 (1998).
[15] R. Hirn, R. Benz, and T. M. Bayerl, Phys. Rev. E **59**, 5987 (1999).
[16] M. F. Hildenbrand and T. M. Bayerl, Biophys. J. **88**, 3360 (2005).
[17] C. R. Safinya, D. Roux, G. S. Smith, S. K. Sinha, P. Dimon, N. A. Clark, and A. M. Bellocq, Phys. Rev. Lett. **57**, 2718 (1986).
[18] J. Nagle, R. Zhang, S. Tristram-Nagle, W. Sun, H. Petrache, and R. Suter, Biophys. J. **70**, 1419 (1996).
[19] Y. Lyatskaya, Y. Liu, S. Tristram-Nagle, J. Katsaras, and J. F. Nagle, Phys. Rev. E **63**, 011907 (2001).
[20] T. Salditt, C. Münster, U. Mennicke, C. Ollinger, and G. Fragneto, Langmuir **19**, 7703 (2003).
[21] G. Pabst, M. Rappolt, H. Amenitsch, and P. Laggner, Phys. Rev. E **62**, 4000 (2000).
[22] V. I. Gordeliy, V. Cherezov, and J. Teixeira, Phys. Rev. E **72**, 061913 (2005).
[23] S. H. Chen, C. Y. Liao, H. W. Huang, T. M. Weiss, M. C. Bellisent-Funel, and F. Sette, Phys. Rev. Lett. **86**, 740 (2001).
[24] M. C. Rheinstädter, C. Ollinger, G. Fragneto, F. Demmel, and T. Salditt, Phys. Rev. Lett. **93**, 108107 (2004).
[25] M. C. Rheinstädter, T. Seydel, F. Demmel, and T. Salditt, Phys. Rev. E **71**, 061908 (2005).
[26] C. Münster, T. Salditt, M. Vogel, R. Siebrecht, and J. Peisl, Europhys. Lett. **46**, 486 (1999).
[27] N. Chu, N. Kucerka, Y. Liu, S. Tristram-Nagle, and J. F. Nagle, Phys. Rev. E **71**, 041904 (2005).
[28] B. Frick and M. Gonzalez, Physica B **301**, 8 (2001).
[29] G. Pabst, J. Katsaras, V. A. Raghunathan, and M. Rappolt, Langmuir **19**, 1716 (2003).